Journal of Solid State Chemistry **150,** 383–390 (2000)
doi:10.1006/jssc.1999.8611, available online at http://www.idealibrary.com on IDEAL®

Atomic and Magnetic Long-Range Orderings in BaLa*M*RuO$_6$ (*M* = Mg and Zn)

Kun-Pyo Hong,* Young-Hyun Choi,† Young-Uk Kwon,†,[1] Duk-Young Jung,† Jeong-Soo Lee,* Hae-Sub Shim,* and Chang-Hee Lee*

*Korea Atomic Energy Research Institute, Taejon, 305-600, Korea; and †Department of Chemistry, Sungkyunkwan University, Suwon, 440-746, Korea

Received October 12, 1999; in revised form December 2, 1999; accepted December 13, 1999

The crystal structures of double perovskite BaLa*M*RuO$_6$ (*M* = Mg, Zn) obtained from the refinements on both X-ray and neutron diffraction data, different from those reported previously that used either X-ray or neutron diffraction data alone, are reported. The room temperature X-ray and neutron data were refined with a model in the tetragonal space group *I*4/*m* (*a* = 5.6230(4), *c* = 7.964(1) Å, *V* = 251.81(4) Å^3 for *M* = Mg; *a* = 5.6521(3), *c* = 7.9987(9) Å, *V* = 255.53(3) Å^3 for *M* = Zn). The low-temperature neutron diffraction data of the two compounds are also refined in the same space group (*a* = 5.6156(4), *c* = 7.953(1) Å, *V* = 250.80(4) Å^3 for *M* = Mg at 13 K; *a* = 5.6418(4), *c* = 7.981(1) Å, *V* = 254.03(4) Å^3 for *M* = Zn at 10 K). Both compounds show almost complete ordering of *B*-site atoms (*M*/Ru). For both compounds, the low-temperature neutron diffraction data below about 20 K showed magnetic diffraction peaks that could be accounted for with a Type I antiferromagnetic ordering of Ru spins in an atomically ordered double perovskite structure. These compounds showed discrepancies between field cooled and zero field cooled magnetization data below the antiferromagnetic ordering temperatures. © 2000 Academic Press

Key Words: **atomic ordering; antiferromagnetic ordering; crystal structure; perovskite; oxide, ruthenium.**

INTRODUCTION

Double perovskites of the general formula $A_2(B, B')O_6$ have attracted continued interest in their synthesis and physical properties, especially magnetism (1). For example, Sr_2FeMoO_6 was reported to exhibit magnetoresistance properties (2) and a superlattice of $LaCrO_3$–$LaFeO_3$ (La_2CrFeO_6) was reported to show high T_c ferromagnetism (3).

Double perovskites containing Ru^{5+} have been studied rather extensively (4–11). Especially, Battle and his colleagues have studied compounds for different combinations of *A* and *B* atoms, and found that the Ru–O–O–Ru interactions generally have strong transfer integrals, *b*. The magnetic properties of these materials strongly depend on the strength of the transfer integral which, in turn, can be influenced by the crystal structures (4–6).

Fernandez *et al.* reported on the synthesis and magnetic properties of compounds of the general formula BaLa*M*RuO$_6$ (*M* = Mg, Fe, Co, Ni, Zn) (11). They reported that all of the compounds except *M* = Fe had superstructures with doubled unit cells in a cubic space group, *Fm*3*m*, based on their X-ray diffraction data. However, using room-temperature and low-temperature neutron diffraction methods, Battle *et al.* reported that the *M* = Zn phase had a monoclinic structure with disordered Zn/Ru atoms (4).

In order to resolve the discrepancy in the literature on the BaLaZnRuO$_6$ compound, we have undertaken X-ray and neutron diffraction studies on this compounds. Also, we have studied the BaLaMgRuO$_6$ compound for comparison. There are several reasons for us to choose the Mg compound for this purpose. First, unlike the other *M* atoms in the paper of Fernandez *et al.*, there is no ambiguity of the oxidation states on Mg^{2+} and Zn^{2+} eliminating possibility of lower oxidation state of Ru than 5+. Second, Mg^{2+} and Zn^{2+} ions have very close ionic sizes so the difference in crystal structures of the two compounds would be minimal. Third, the absence of any unpaired *d* electrons that may interact with those of Ru can provide a clear view on the magnetic interactions between the Ru ions in the structure. We have employed both X-ray and neutron diffraction techniques, which led us to different crystal structures, in the tetragonal *I*4/*m* space group, from those of the two papers mentioned above, which used either one of the diffraction techniques only. For these particular examples, simultaneous application of both diffraction techniques crucially played complementary roles in leading to the actual crystal structures.

EXPERIMENTAL

Stoichiometric amounts of $BaCO_3$, La_2O_3, RuO_2, $(MgCO_3)_4Mg(OH)_2 \cdot 5H_2O$, and ZnO were ground

[1]To whom correspondence should be addressed. E-mail: ywkwon@chem.skku.ac.kr.

0022-4596/00 $35.00

together, pressed into pellets, and reacted at 900°C for 12 h, 1000°C for 40 h, and 1150°C for 30 h. The first 900°C reaction step was necessary to prevent any loss of the volatile RuO_2 during the reactions. Intermittent grinding and pelleting cycles were carried out to ensure the homogeneity of the samples.

Rietveld structural refinements of the compounds are performed on the powder X-ray and neutron diffraction data. The room-temperature X-ray data were collected on a Rigaku diffractometer equipped with a monochromated Cu$K\alpha$ radiation, in the 2θ range from 10° to 120°. The conditions of 0.02° of step size and 7 s scan per step were used for the data collections. The neutron diffraction data were collected using the HRPD diffractometer on the research reactor HANARO at KAERI. Thermal neutrons monochromated with a Ge(331) single crystal, $\lambda = 1.8343$ Å were used for the experiments. The data were collected in the 2θ range of 0° to 160°. A vanadium can was used as the sample holder for the room-temperature data collections. The low-temperature experiments were performed on a sample contained in a vanadium can, which was, in turn, encased in a He-filled aluminum canister.

The FULLPROF program suite (12) was used for the structural refinements on both the X-ray and neutron data. Six parameters of polynomial background parameters, pseudo-Voigt type profile function with three parameters, asymmetric peak shape function with four terms, and three term anisotropic strain parameters were used in the refinements. The sample holders used for the neutron diffraction gave spurious peaks at $2\theta = 50$–51° and 76.2–76.8° regions in the room temperature data and additional peaks at 13–14°, 50–55°, 76–81°, 130.5–132° in the low-temperature data, which were excluded in the refinements.

Magnetic susceptibility data were obtained from a SQUID (KBRI) at an applied field of 1000 G. Both field cooling (FC) and zero field cooling (ZFC) data in the 5–300 K temperature range were recorded. For both experiments, the sample was cooled to 5 K with (FC) or without (ZFC) an applied field and the magnetization data were recorded while warming up to room temperature.

RESULTS AND DISCUSSION

The room-temperature X-ray powder diffraction patterns of our $BaLaMRuO_6$ (M = Mg and Zn) compounds could be indexed in a cubic unit cell with doubled lattice parameters in agreement with Fernandez *et al.* (11). They discussed that the superstructures were due to the *B*-site atomic orderings in their samples. Therefore, we have initially refined our X-ray powder diffraction data in the supposed $Fm3m$ to get acceptable agreement factors ($R_p = 9.52\%$, $R_{wp} = 13.5\%$, $R_B = 5.07\%$ for M = Mg; $R_p = 9.03\%$, $R_{wp} = 12.9\%$, $R_B = 5.33\%$ for M = Zn compounds). Also, the M/Ru occupancy factor refinements strongly suggest that the M/Ru atoms are ordered in both phases. The intensities of (111) peaks at $2\theta = 19.2°$ of the X-ray diffraction patterns (Fig. 1) are particularly sensitive to the degree of atomic orderings; the intensities calculated for the random distribution models were close to zero. However, the same structural model could not account for the room-temperature neutron diffraction data. The peak intensities of all odd *hkl* reflections, such as (311), (531), and (533), were calculated to be much weaker than the observed while the other peaks could be well fitted.

Because neutron diffraction technique is more sensitive to the parameters of oxygen atoms than X-ray, the relatively

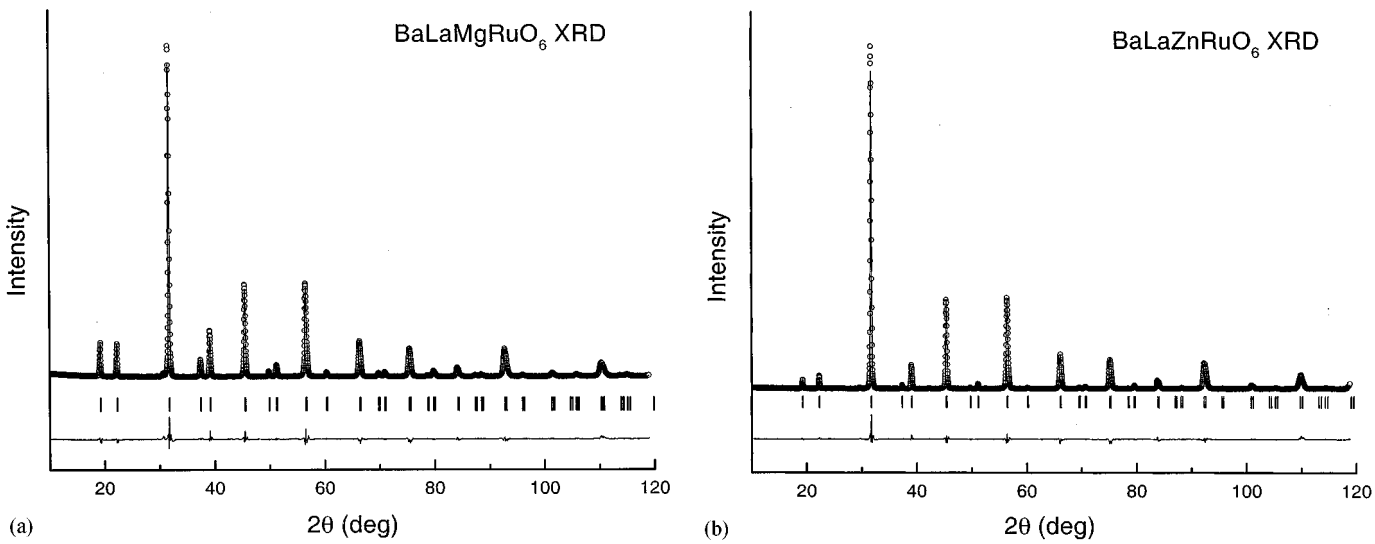

FIG. 1. Rietveld refinement results on the room-temperature X-ray diffraction patterns of (a) $BaLaMgRuO_6$ and (b) $BaLaZnRuO_6$.

good agreement for the X-ray data and poor agreement for the neutron data with the $Fm3m$ model can be explained because the metallic positions are close to those of the ideal cubic structure but the oxygen positions deviate from the ideal model. Similar observations were made for the Sr_2FeTaO_6 compound, for which the neutron diffraction data led to a $GdFeO_3$-type structure in the orthorhombic $Pbnm$ space group while the X-ray powder pattern could well be indexed with a cubic unit cell (13). However, this orthorhombic structural model is not suitable for our cases because this model does not allow ordering of M/Ru atoms. The atomic ordering is possible by further lowering the symmetry to $P2_1/n$. Indeed, the crystal structures of related double perovskites of Ru^{5+} such as Ca_2LaRuO_6 (6) and Sr_2YRuO_6 (5) were refined in this monoclinic space group and were reported to have B-site atomic orderings. Our powder patterns, both low temperature and 300 K, of the Mg and Zn phases also could be refined in this space group with ordered M/Ru atoms, though some constraints on the parameters were required to avoid divergent results.

However, the apparent high symmetry implied by the powder patterns led us to explore other space groups. Because the structural models in the cubic space group could account for the X-ray powder patterns well to some extent and produced only a few peak intensities of the neutron diffraction patterns that showed disagreement, we considered that a subgroup of $Fm3m$ could be the correct group. Therefore, we have considered all of the five direct nonisomorphic subgroups of $Fm3m$ and their subgroups with the following criteria. The correct subgroup must allow M/Ru ordering and place all the metallic elements as in the $Fm3m$ model. It also must allow the oxygen atoms to move from the positions in the $Fm3m$ model and still maintain the octahedral geometry around the M/Ru atoms. There were only two second generation subgroups, $R\bar{3}$ and $I4/m$, that satisfied these criteria. We have attempted both space groups for the structural refinements and found that both the low-temperature and 300-K neutron diffraction data of both Mg and Zn phases could be well refined in the $I4/m$ structural models. In contrast, the refinements in the $R\bar{3}$ model were unstable and the final results, with some restrictions on the parameters, yielded results with poorer agreement factors than those with the $I4/m$ model. We, therefore, have chosen the $I4/m$ structures as the correct structures, and the details are reported here. However, we cannot simply rule out the $R\bar{3}$ space group by just comparing the agreement factors or the behavior of the refinements. This is mainly because the structural distortions are only reflected in the intensities of peaks with all odd hkl indices in the neutron diffraction patterns, and there are only a few such peaks. Nevertheless, it is certain that the crystal structure of our compounds is very close to that of $Fm3m$. The refinements in the monoclinic space group $P2_1/n$ also produced good agreements, although they suffered from instability of the refinement, but the essential features are identical to those of $I4/m$ with no improvement of the agreement factors. The validity of the high symmetry nature of the compounds is partly supported by the fact that the low temperature powder patterns do not reveal any additional peaks or peak splitting except for the very weak magnetic peaks at low angles.

In Tables 1 and 2, we summarize the refinement results of the Mg and Zn phases based on the simultaneous refinements of both X-ray and neutron diffraction data at room temperature and on the neutron data at low temperature. The calculated powder patterns are compared with the observed patterns in Figs. 1–3. The slightly poorer agreements for the low-temperature data than the 300-K data, are mainly because the former employed shorter counting times.

The relative occupancies of M/Ru on the B-sites were obtained from the simultaneous refinements of the X-ray and neutron data at 300 K and these were used as fixed parameters for the refinements of the low-temperature neutron data. The occupancy refinements for both phases suggest that the M/Ru atoms are almost completely ordered in both compounds (the proportions of M in M site (and Ru in Ru site) are 96.4(3)% for the Mg and 99.3(8)% for the Zn compounds). Therefore, the structures can be classified as the rock-salt type according to the scheme by Poeppelmeier (1). One must be cautious in taking the refined occupancies,

TABLE 1

Results of the Rietveld Crystal Structure Refinements of $BaLaMgRuO_6$ from the Simultaneous Refinements of the X-Ray and Neutron Diffraction Data at 300 K and Single-Pattern Neutron Diffraction Data at 13 K

Temperature	300 K		13 K
Space group		$I4/m$	
Type of data	X-ray	Neutron	Neutron
a (Å)		5.6230(4)	5.6156(4)
c (Å)		7.964(1)	7.953(1)
Atoms			
Ba/La, B_{iso}		1.15(3)	0.32(4)
Mg, B_{iso}		0.87(3)	0.30(5)
Occupancy of Mg (%)		96.4(3)	
Ru, B_{iso}		0.87(3)	0.30(5)
Occupancy of Ru (%)		96.4(3)	
O1, z		0.253(6)	0.253(6)
B_{iso}		1.93(5)	1.7(1)
O2, x		0.224(3)	0.226(3)
y		0.279(3)	0.283(3)
B_{iso}		1.93(5)	1.03(7)
R_p	0.089	0.046	0.064
R_{wp}	0.129	0.058	0.084
χ^2	4.81	2.05	3.01
R_B	0.045	0.056	0.049
R_F	0.031	0.045	0.031

TABLE 2

Results of the Rietveld Crystal Structure Refinements of $BaLaZnRuO_6$ from the Simultaneous Refinements of the X-Ray and Neutron Diffraction Data at 300 K and Single-Pattern Neutron Diffraction Data at 10 K

Temperature		300 K	13 K
Space group		*I*4/*m*	
Type of data	X-ray	Neutron	Neutron
a (Å)		5.6521(3)	5.6418(3)
c (Å)		7.9987(9)	7.981(1)
Atoms			
Ba/La, B_{iso}		1.14(3)	0.40(5)
Zn, B_{iso}		0.95(3)	0.29(6)
Occupancy of Zn (%)		99.3(8)	
Ru, B_{iso}		0.95(3)	0.29(6)
Occupancy of Ru (%)		99.3(8)	
O1, *z*		0.254(4)	0.254(8)
B_{iso}		2.16(4)	2.9(2)
O2, *x*		0.226(2)	0.225(3)
y		0.286(2)	0.285(3)
B_{iso}		2.18(4)	1.04(8)
R_p	0.087	0.064	0.070
R_{wp}	0.126	0.082	0.090
χ^2	2.57	3.04	3.52
R_B	0.045	0.060	0.049
R_F	0.034	0.051	0.036

however, because they tend to show different values depending on the data used for the refinements as well as refinement conditions. For example, if the X-ray data were used alone, the occupancy factors were lowered by 5–10%, implying partial mixing. Because these compounds were synthesized at high temperatures, the entropy factor would favor some degree of disorder and we cannot rule out the possibility of partial disorder although the refinements resulted in complete orderings in these compounds. The reported structure of $BaLaZnRuO_6$ compound with disordered Zn and Ru atoms (4) may be because the neutron scattering factors of Zn (0.5680×10^{-12} cm) and Ru (0.7030×10^{-12} cm) are not much different from each other and cannot be well distinguished by neutrons alone. In fact, we have also experienced difficulty in refining the *M*/Ru occupation factors on the neutron diffraction data alone. The atomic orderings occur when the ionic sizes and charges of the two *B* ions are significantly different (1). These conditions are well satisfied by our Mg^{2+}/Ru^{5+} and Zn^{2+}/Ru^{5+} cases. The effective ionic radii of Mg^{2+} and Zn^{2+} are 0.72 and 0.74 Å and that of Ru^{5+} is 0.565 Å (14), and the charge difference is substantial. It is also well established that the Ru in our compounds is Ru^{5+} from the magnetic susceptibility data in the literature (11) as well as our own data (below). The smaller degree of ordering for the Mg compound can be explained due to the smaller difference of the ionic size with that of Ru^{5+} than for the Zn compound.

The crystal structures can be best described in terms of Glazer's MO_6 octahedron rotation scheme (15–17). According to this scheme, our samples can be denoted as $a^0a^0c^-$, meaning that the adjacent octahedra are not tilted from each other as in the ideal cubic structure when viewed along the [110] direction while they are tilted alternatively along the [001]-direction (Fig. 4). Besides the tilting of the RuO_6 octahedra, the structure would be exactly the same as in the ideal cubic structure.

The bond distances from the 300-K data refinements were calculated as shown in Tables 3 and 4. The Ru–O bond

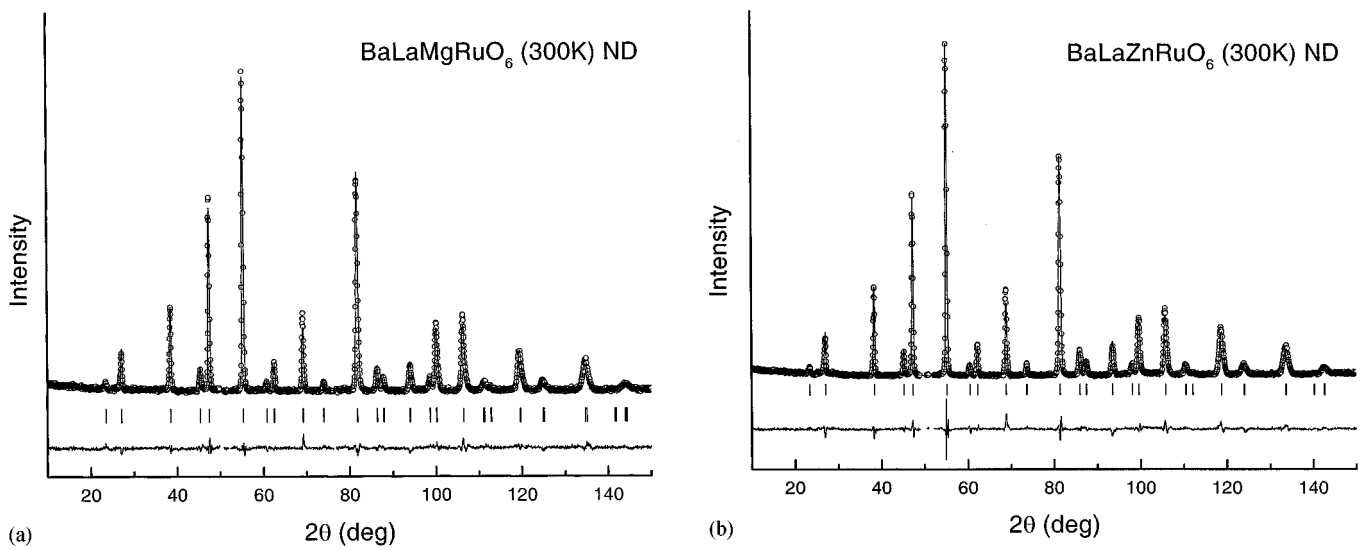

FIG. 2. Rietveld refinement results on the room-temperature neutron diffraction patterns of (a) $BaLaMgRuO_6$ and (b) $BaLaZnRuO_6$.

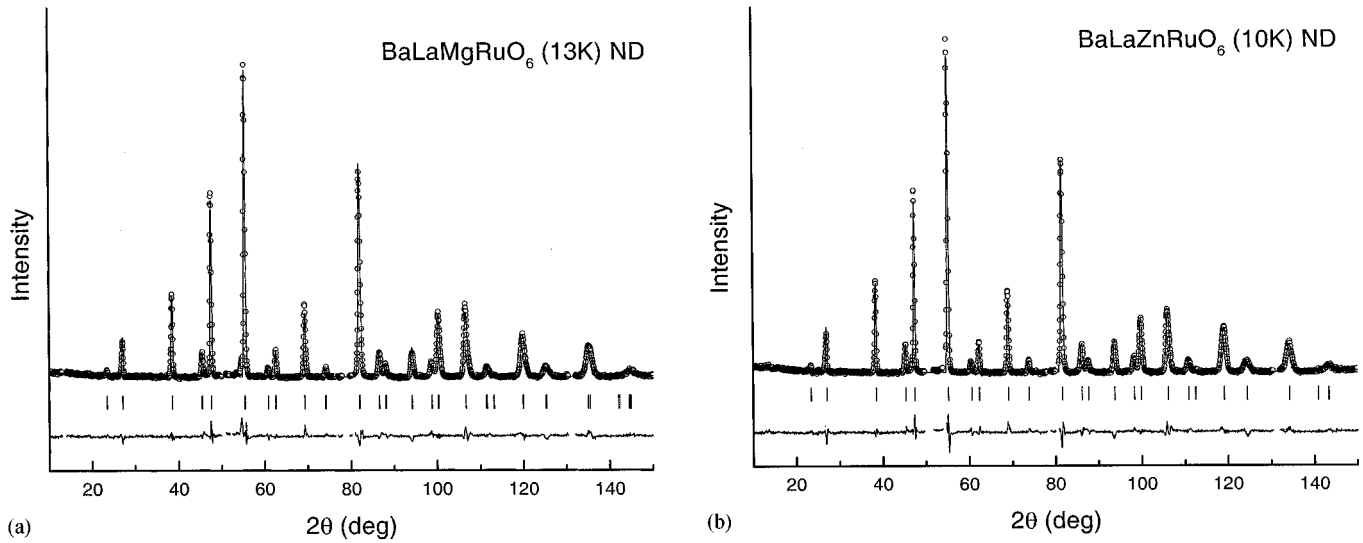

FIG. 3. Rietveld refinement results on the low-temperature neutron diffraction patterns of (a) BaLaMgRuO$_6$ at 13 K and (b) BaLaZnRuO$_6$ at 10 K.

distances of the both Mg and Zn compounds are identical within the standard deviations and uniform at 1.96–1.98 Å. These values are comparable to those in the literature ranging from 1.93 to 1.99 Å (4–6). The M–O bond distances for Mg and Zn are uniform at 2.01 and 2.03–2.06 Å, respectively, the latter being slightly larger reflecting than Zn^{2+} is larger than Mg^{2+}. The bond angles around the M/Ru atoms are all symmetry constrained to ideal values of 90° or 180°. Therefore, the RuO$_6$ and MO$_6$ octahedra in the present compounds can be considered to be ideal octahedra. The M/Ru–O bond distances remained unchanged upon cooling within the standard deviations. The main changes with temperature are on the Ba/La–O distances as can be seen in Tables 3 and 4.

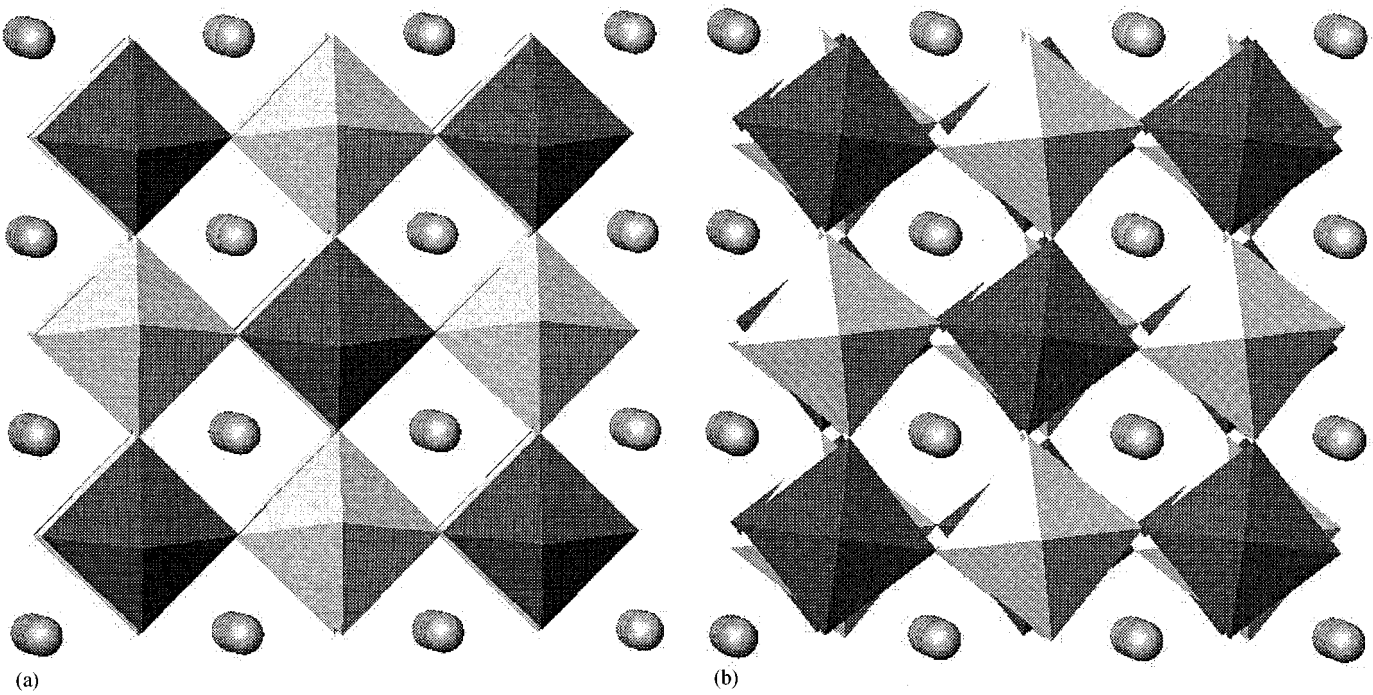

FIG. 4. Crystal structure of BaLaMRuO$_6$ (M = Mg and Zn) viewed along the (a) [110] and (b) [001] directions.

TABLE 3
Bond Distances and Angles of $BaLaMgRuO_6$ from Room-Temperature X-Ray and Neutron Diffraction Data Refinements and 13 K Neutron Diffraction Data Refinements

300 K			
Ba/La–O1 (×4)	2.8116(4)	Mg–O1 (×2)	2.01(5)
–O2 (×4)	2.97(1)	–O2 (×4)	2.01(2)
–O2 (×4)	2.67(1)	Ru–O1 (×2)	1.97(5)
		–O2 (×4)	1.98(2)
Mg–O1–Ru	180(2)	Mg–O2–Ru	167.6(7)
13 K			
Ba/La–O1 (×4)	2.8078(4)	Mg–O1 (×2)	2.01(3)
–O2 (×4)	2.980(9)	–O2 (×4)	2.04(1)
–O2 (×4)	2.649(8)	Ru–O1 (×2)	1.96(3)
		–O2 (×4)	1.96(1)
Mg–O1–Ru	180(3)	Mg–O2–Ru	166.5(5)

The magnetic susceptibility data of the Mg and Zn samples are shown in Fig. 5. Both compounds show antiferromagnetic orderings below 20 K. Above the antiferromagnetic ordering temperature, T_N, both compounds show typical Curie–Weiss behavior in agreement with the previous reports. The data were fit to the Curie–Weiss law, $\chi = C/(T - \theta)$, where C is the Curie constant and θ is the Weiss temperature, to get $\mu_{eff} = 4.10$ BM and $\theta = 295$ K for the Mg and $\mu_{eff} = 4.19$ BM and $\theta = 216$ K for the Zn compounds. Fernandez *et al.* reported that their Mg and Zn samples showed Curie–Weiss behavior above T_N up to over 700°C. Magnetic moments of 3.85 and 3.84 BM per Ru^{5+} for the Mg and Zn compounds, respectively, were calculated, close to the spin only value of 3.87 BM for the t_{2g}^3 configuration (11). In fact, spin only values are not expected for 4*d* transition metal ions because of large spin-orbit coupling which, for the present t_{2g}^3 case, should reduce the effective magnetic moment. On the contrary, the magnetic moments of our samples are even larger than the spin-only value. For comparison, Ba_2LaRuO_6, and Ca_2LaRuO_6 were reported to have effective magnetic moments $\mu_{eff} = 4.27$ and 4.00 BM, which are close to ours (6). The discrepancy from the prediction based on the crystal field theory was explained by the action of itinerant electrons as the transfer integral b approaches b_m in the $b_c < b < b_m$ region. The large values of the ratio $\theta/T_N > 10$ for Ba_2LaRuO_6 and Ca_2LaRuO_6 are also a good diagnosis that b is close to b_m, which again is the case of our Mg and Zn compounds with $\theta/T_N = 16$ and 11, respectively. Therefore, the magnetic properties of our $BaLaMRuO_6$ (M = Mg, Zn) compounds can be explained as being the result of itinerant electrons of Ru^{5+} that interact with one another strongly to give rather large transfer integrals. The very close crystallographic dimensions of the two compounds result in similar magnetic properties.

TABLE 4
Bond Distances and Angles of $BaLaZnRuO_6$ from Room-Temperature X-Ray and Neutron Diffraction Data Refinements and 10 K Neutron Diffraction Data Refinements

300 K			
Ba/La–O1 (×4)	2.8263(5)	Zn–O1 (×2)	2.03(3)
–O2 (×4)	3.00(1)	–O2 (×4)	2.06(1)
–O2 (×4)	2.663(8)	Ru–O1 (×2)	1.96(3)
		–O2 (×4)	1.96(1)
Zn–O1–Ru	180(1)	Zn–O–Ru	166.3(5)
10 K			
Ba/La–O1 (×4)	2.8215(6)	Zn–O1 (×2)	2.02(6)
–O2 (×4)	3.00(1)	–O2 (×4)	2.05(2)
–O2 (×4)	2.66(1)	Ru–O1 (×2)	1.97(6)
		–O2 (×4)	1.97(2)
Zn–O1–Ru	180(2)	Zn–O2–Ru	166.1(7)

The antiferromagnetic nature of magnetic ordering is also evident from the low-temperature neutron diffraction data (Fig. 6). Although very weak, magnetic peaks grew as the temperature was lowered for both samples. The indices of these magnetic peaks, (001), (100), (111), (102), violate the systematic absence condition of the *I*-centered chemical unit cell indicating that there is a long-range antiferromagnetic ordering. Because the magnetic scattering factor for Ru^{5+} is not available, the magnetic structure could not be refined. Nevertheless, we have attempted some refinements on the magnetic structures using the scattering factor of Ru^{3+} just to see how the Ru^{5+} spins are ordered. The best model we have obtained is Type I, in which there are parallel spins within the *ab* plane and the spins of adjacent planes are antiparallel. The (001) and (100) magnetic reflections in the compounds suggest that the Ru^{5+} spins are not parallel to the *c* axis or to the *ab* plane. The same type magnetic structures were reported on *B*-site ordered Ca_2LaRuO_6 and Sr_2YRuO_6 compounds (5, 6).

In their paper on the disordered structure of $BaLaZnRuO_6$ compound, Battle *et al.* reported its magnetic structure as Type *A* (4). In the Type *A* magnetic structure, there are parallel spins within a plane and adjacent planes have antiparallel spins, very similar to the Type I structure except that Type *A* is based on the primitive perovskite structure with no *B*-site ordering and Type I is based on the doubled superstructure. In order to explain why the magnetic structure was Type *A*, they invoked the possibility of short-range ordering of Zn and Ru forming a large population of Ru–O–Zn connectivity, a feature which is already present in our crystal structure.

As shown in Fig. 5, both Mg and Zn compounds show divergent ZFC and FC data below T_N, a problem which has not been addressed previously. Similar magnetic behavior was reported on Sr_2FeSbO_6 (13). In this compound, the

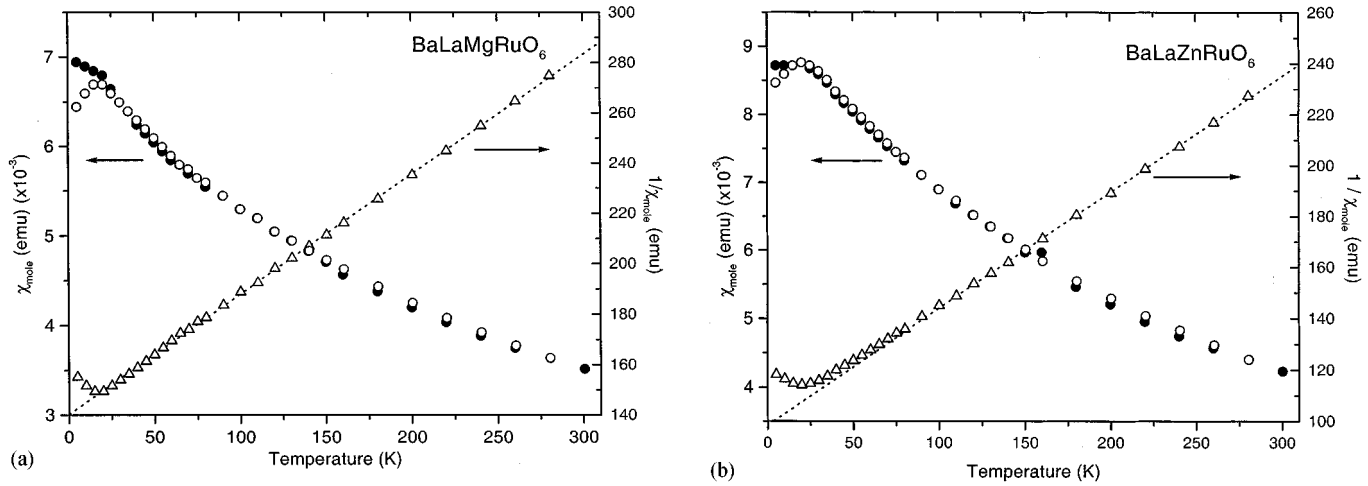

FIG. 5. Magnetic susceptibility data and Curie–Weiss fit of (a) BaLaMgRuO$_6$ and (b) BaLaZnRuO$_6$.

Fe^{3+} and Sb^{5+} ions are ordered in the *B*-site by about 80%, and show a long-range magnetic ordering, as revealed from low-temperature neutron diffraction data, and a discrepancy between ZFC and FC data below T_N, 37 K. This magnetic behavior was explained as that there is an antiferromagnetic backbone composed of the Fe ions in the one sites and the disordered Fe ions form antiferromagnetic clusters whose movement becomes frozen below T_N. This explanation does not seem to apply well to our compounds that have almost perfectly ordered structures. However, because of the uncertainties associated with the refined occupancy factors depending on the refinement conditions as described above, this possibility may not be completely ruled out. The other possibility is the competition between different types of Ru–O–O–Ru interactions present in our compounds. Because of the tilting of the octahedra along the *c* axis, the Ru–O–*M* bond angle within the *ab* plane deviates from 180°, whereas the angle along the *c* axis is strictly 180°. Therefore, the Ru–O–O–Ru interaction within the *ab* plane is mediated by two non-180° Ru–O–*M* bond angles, and the angle along the *c* direction is mediated by a 180° and a non-180° Ru–O–*M* interaction. If the bond angles were strictly 180°, these interactions would be antiferromagnetic. Deviation from 180° of a bond angle renders a ferromagnetic component. Therefore, the antiferromagnetic interactions within the *ab* plane are weaker than those

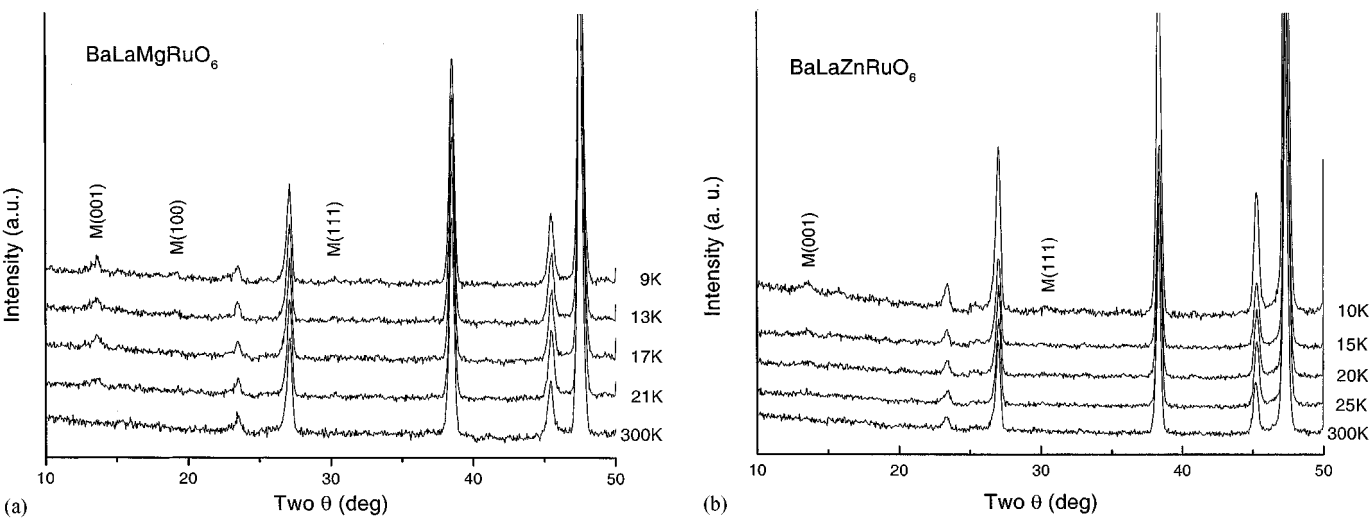

FIG. 6. Evolution of the magnetic peaks in the low-temperature neutron diffraction patterns of (a) BaLaMgRuO$_6$ and (b) BaLaZnRuO$_6$.

involving the interactions in the c direction. This is consistent with the Type I magnetic structure deduced from the low-temperature neutron diffraction data. However, the inherent antiferromagnetic nature of the interaction within the ab plane will compete with this magnetic ordering, resulting in frustrated spins below T_N.

In conclusion, we have performed both X-ray and neutron diffraction studies on $BaLaMRuO_6$ compounds. The M and Ru atoms are ordered in the B site and the structures are slightly distorted from the ideal cubic to tetragonal structures. Our study demonstrates the importance of using both X-ray and neutron diffraction techniques in elucidating crystal structures of some compounds by showing that X-ray alone could lead to a cubic structure and that neutron alone could lead to a random distribution of the B-site atoms.

ACKNOWLEDGMENTS

Financial support for this research was from Korea Science and Engineering Foundation (K-N96048). Neutron diffraction experiments were performed at KAERI operated under the Nuclear Research and Development program by the Ministry of Science and Technology, Korea. We thank Korea Basic Science Institute for access to SQUID for magnetic measurements.

REFERENCES

1. M. T. Anderson, K. B. Greenwood, G. A. Taylor, and K. R. Poeppelmeier, *Prog. Solid State Chem.* **22,** 197 (1993).
2. K. L. Kobayashi, T. Kimura, H. Sawada, K. Terakura, and Y. Tokura, *Nature* **395,** 677 (1998).
3. K. Ueda, H. Tabata, and T. Kawai, *Science* **280,** 1064 (1998).
4. P. D. Battle, T. C. Gibb, C. W. Jones, and F. Studer, *J. Solid State Chem.* **78,** 281 (1989).
5. P. D. Battle and W. J. Macklin, *J. Solid State Chem.* **52,** 138 (1984).
6. P. D. Battle, J. B. Goodenough, and R. Price, *J. Solid State Chem.* **46,** 234 (1983).
7. S. H. Kim and P. D. Battle, *J. Solid State Chem.* **114,** 174 (1995).
8. S. H. Kim and P. D. Battle, *J. Magn. Magn. Mate.* **123,** 273 (1993).
9. P. D. Battle, S. K. Bollen, and A. V. Powell, *J. Solid State Chem.* **99,** 267 (1992).
10. M. P. Attfield, P. D. Battle, S. K. Bollen, S. H. Kim, A. V. Powell, and M. Workman, *J. Solid State Chem.* **96,** 344 (1992).
11. I. Fernandez, R. Greatrex, and N. N. Greenwood, *J. Solid State Chem.* **32,** 97 (1980).
12. J. Rodriguez-Carvajal, "Fullprof.99," Version 0.1 April 1999 (JRC-LLB) (Beta-Test); the software used was wmfp99.exe that enabled simultaneous refinements of X-ray and neutron diffraction data.
13. E. J. Cussen, J. F. Vente, P. D. Battle, and T. C. Gibb, *J. Mater. Chem.* **7,** 459 (1997).
14. R. D. Shannon, *Acta Crystallogr. Sect. A* **32,** 751 (1976).
15. A. M. Glazer, *Acta Crystallogr. Sect. A* **31,** 756 (1975).
16. P. M. Woodward, *Acta Crystallogr. Sect. B* **53,** 32 (1997).
17. P. M. Woodward, *Acta Crystallogr. Sect. B* **53,** 44 (1997).